Scientific Reports

https://doi.org/10.1038/s41598-026-45608-9

Article in Press

γ-Tocotrienol inhibition of galectin-3 expression, distribution and oligomerization in highly metastatic breast cancer cells

Received: 21 November 2025

Accepted: 20 March 2026

Published online: 26 March 2026

Cite this article as: Grazier J.J. & Sylvester P.W. γ-Tocotrienol inhibition of galectin-3 expression, distribution and oligomerization in highly metastatic breast cancer cells. *Sci Rep* (2026). https://doi.org/10.1038/s41598-026-45608-9

Jessie J. Grazier & Paul W. Sylvester

Original Research Article

Second Revision March 18, 2026

γ-Tocotrienol Inhibition of Galectin-3 Expression, Distribution and Oligomerization in Highly Metastatic Breast Cancer Cells

Jessie J. Grazier and Paul W. Sylvester*

College of Pharmacy, University of Louisiana at Monroe

1800 Bienville Drive, Monroe LA 71201, USA

*Corresponding Author: Dr. Paul W. Sylvester,

College of Pharmacy,

University of Louisiana at Monroe,

1800 Bienville Drive

Monroe, LA 71201

Telephone : 318-342-1958

Fax : 318-342-1737

Email : sylvester@ulm.edu

Running Title: γ-Tocotrienol, Galectin-3 and Metastatic Breast Cancer

Key Words: γ-Tocotrienol, Galectin-3, EMT, Metastasis, Breast Cancer

ABSTRACT:

Experimental studies were conducted to compare the relative effects of γ-tocotrienol, a natural isoform within the vitamin E family of compounds, with established galectin-3 inhibitor β-lactose, on galectin-3 levels and distribution in highly metastatic human MDA-MB-231, and mouse +SA and TS/A breast cancer cell lines. In contrast to β-lactose, γ-tocotrienol displays a dual-mode binding profile with the carbohydrate recognition domain and hydrophobic pocket located on galectin-3, as determined using Schrödinger molecular modeling. However, treatment with either γ-tocotrienol or β-lactose induces a significant decrease in galectin-3 expression, oligomerization, and a corresponding decrease in fibronectin fibril and lamellipodial protrusion formation, an indication of treatment-induced reversal in epithelial-mesenchymal transition (EMT). These same treatments also caused a significant decrease in galectin-3 Fluorescence Resonance Energy Transfer (FRET) signaling, as compared to the control group, demonstrating the intricate role of galectin-3 in modulating EMT in metastatic breast cancer cells. Combined treatment of doxorubicin with either γ-tocotrienol or β-lactose results in a large increase in doxorubicin levels in the nuclei of metastatic breast cancer cells, the primary site of action for this chemotherapeutic agent. Taken together these findings demonstrate that γ-tocotrienol-induced reversal of EMT in metastatic breast cancer cells is mediated, at least in part, by a disruption in the galectin-3 expression, distribution and function.

INTRODUCTION

Cancer metastasis remains a major challenge in oncology, contributing significantly to morbidity and mortality in cancer patients (1). Galectin-3 is a β-galactoside-binding lectin that plays a critical role in the modulation of epithelial-mesenchymal transition (EMT) and metastatic phenotypic expression in various cancer cell types (1). Specifically, elevated galectin-3 expression is correlated with a reduction in E-cadherin (epithelial cell marker) and a corresponding elevation in vimentin (mesenchymal cell marker) expression, both of which are hallmarks of EMT (2, 3). These specific cell marker transitions are associated with a weakening in cell-cell adhesion and the promotion of tumor cell migration and invasion (4). Galectin-3 also interacts with transmembrane cell adhesion receptors, such as integrins, to further promote the transition to a mesenchymal state and facilitate cytoskeletal reorganization and cellular motility (1). Furthermore, galectin-3 directly enhances the expression of a metastatic phenotype through its ability to augment transendothelial invasion, allowing cancer cells to breach vascular barriers and ultimately invade distant tissues and organs (5). Given the multifaceted role galectin-3 plays in tumor progression, this β-galactoside-binding lectin has recently attracted great interest as a potential therapeutic target in the treatment of metastatic cancers. Therefore, it was hypothesized that attenuation of galectin-3 expression and function may provide significant benefit for impeding EMT, reducing metastatic burden, and enhancing the effectiveness of existing anticancer therapies.

Previous studies have demonstrated that γ-tocotrienol, a natural isoform in the vitamin E family of compounds, is a potent anticancer agent that inhibits breast cancer EMT, invasiveness and metastatic progression (2, 6-8). The exact mechanism(s) mediating γ-tocotrienol anticancer activity is currently unknown, but does involve a wide variety of signaling pathways. γ-Tocotrienol treatment has been shown to attenuate EGF-dependent mitogenic signaling pathways,

particularly MAPK, PI3K/Akt and NFκB among others, which ultimately results in anti-proliferative, pro-apoptotic, anti-angiogenic, anti-metastatic, and pro-autophagic responses, as well as, sensitizing cancer cells to other chemotherapeutic agents (9). Furthermore, these inhibitory effects of γ-tocotrienol are found to occur at treatment doses that have little or no effect on normal mammary epithelial cell growth or viability (10, 11). Since galectin-3 has been shown to play a critical role in the expression of breast cancer cell metastatic phenotype and γ-tocotrienol inhibits metastatic breast cancer cell proliferation, EMT, migration and invasion, studies were conducted to characterize the effects of γ-tocotrienol-dependent modulation of galectin-3 expression, localization and activity in various types of metastatic and non-metastatic breast cancer cells maintained in culture.

RESULTS

Schrödinger Docking Simulations of Galectin-3 Amino Acid Interactions With β-Lactose and γ-Tocotrienol: It is well established that γ-tocotrienol displays potent anticancer activity and reverses epithelial-to-mesenchymal transition (EMT) in a variety of highly malignant breast cancer (9). Since galectin-3 plays a critical role in the promotion of EMT and metastatic phenotypic behavior, it was hypothesized that γ-tocotrienol anticancer effects may be mediated by reducing galectin-3 expression and/or function in highly malignant breast cancer. In addition, β-lactose is a well-established competitive inhibitor of extracellular galectin-3 carbohydrate binding (12). Galectin-3 is a chimeric lectin featuring a C-terminal carbohydrate recognition domain (CRD) that can interact with glycoconjugates and an N-terminal tail that can interact with the hydrophobic pocket of galectin-3 to promote oligomerization. Therefore, computer assisted Schrodinger docking modeling was conducted to compare and contrast galectin-3 amino acid interactions with γ-tocotrienol and β-lactose. The molecular structures of γ-tocotrienol and β-lactose are shown in

(Figure 1A, Top) and (Figure 1B, Top), respectively. Docking analysis of γ-tocotrienol (Figure 1A, Middle) and β-lactose (Figure 1B, Middle) with the galectin-3 protein found several key interactions within the carbohydrate recognition domain (CRD) of galectin-3. Specifically, both γ-tocotrienol (Figure 1A, Middle) and β-lactose (Figure 1B, Middle) preferentially bind to the critical amino acid residues arginine (ARG) and glutamic acid (GLU). The binding affinity of γ-tocotrienol with ARG and GLU within the CRD appears to be further enhanced by the presence of a hydrophobic binding pocket within galectin-3 (Figure 1A, Middle). This binding pocket is characterized by several hydrophobic residues that may facilitate the accommodation of the long hydrophobic side chain of γ-tocotrienol (Figure 1A, Middle). β-Lactose interaction with galectin-3 primarily involved hydrogen bonding with ARG and GLU in the CRD (Figure 1B, Middle). Specifically, the hydroxyl groups of β-lactose form stable hydrogen bonds with the nitrogen atom of ARG, while another hydroxyl group interacted with the carboxyl group of GLU (Figure 1B, Middle). Three-dimensional docking between galectin-3 and γ-tocotrienol and β-lactose are shown in Figure 1A, Bottom and Figure 1B, Bottom, respectively.

Effects of γ-Tocotrienol on Total Galecin-3 Expression Throughout a 0-36-Hour Treatment Period in Highly Malignant Mouse +SA Mammary Tumor Cells: Stain-free visualization of total protein in each lane is shown in Figure 2A. Western blot analysis shows that a 0-36-hour exposure to 5 μM γ-tocotrienol resulted in a time-responsive decrease in galectin-3 expression in highly malignant +SA mouse mammary tumor cells, as compared to the cells in the vehicle-treated control group (Figure 2B). Densiometric analysis of galectin-3 bands following a 0-36 hour treatment exposure to 5 μM γ-tocotrienol shows a significant time-responsive decrease in galectin-3 expression in +SA cells, as compared to the 0 hour vehicle-treatment control group (Figure 2C).

Effects of Triton X-100 Induced Cellular Membrane Permeability on Intracellular and

Extracellular Galectin-3 Visualization in Highly Malignant Mouse +SA Mammary Tumor Cells: Galectin-3 is found to be present in both the intra- and extracellular domains where it functions as a structural protein that binds ligands noncovalently. In the absence of Triton X-100, immunocytochemical antibodies are unable to gain access to intracellular galectin-3 targets, resulting in only the visualization of galectin-3 located in the extracellular matrix surrounding +SA cells (Figure 3A and 3B). In contrast, treatment with 0.4% Triton X-100 was found to increase cell membrane permeability, as evidenced by the visualization of galectin-3 (green) co-localized with DAPI (blue) in the nucleus. However, while treatment with 0.4% Triton X-100 prior to immunocytochemical analysis, increases intracellular galectin-3 labeling and visualization, it also results in the "washing away" of galectin-3 from the extracellular matrix, since membrane structure is disrupted (Figure 3C and 3D). These results demonstrate that only extracellular galectin-3 can be visualized in the absence of Triton X-100 (Figure 3A and 3B), whereas only intracellular galectin-3 can be visualized following exposure to 0.4% Triton X-100 in mouse +SA breast cancer cells (Figure 3C and 3D).

Effects of γ-Tocotrienol on Extracellular Distribution of Galectin-3 in +SA Cells: In the absence of Triton X-100 exposure, +SA cells in the vehicle-treated control group exhibited a widespread, but uneven distribution of galectin-3 within the extracellular matrix surrounding +SA tumor cells (Figure 4A). This distribution pattern is characteristically typical for oligomerization and lattice formation of galectin-3 within the extracellular matrix and is believed to be an indication that galectin-3 plays a vital role in maintaining cell-cell interactions and structural integrity among neighboring cells (13). However, following a 24-hour treatment exposure to 5 μM γ-tocotrienol, a significant shift in galectin-3 localization was observed. Specifically, galectin-3 no longer shows a widespread distribution in the extracellular matrix, but is now redistributed and concentrated

around select individual +SA breast cancer cells (Figure 4B).

Effects of γ-Tocotrienol and β-Lactose on Extracellular Fibronectin Fibril Formation and Galectin-3 Expression in Highly Malignant TS/A Mammary Tumor Cells: Vehicle-treated control TS/A mammary tumor cells show extracellular fibronectin (red) form highly organized fibrils that are arranged on top of the extracellular galectin-3 (green) matrix (Figure 5A). In contrast, exposure to either 6 μM γ-tocotrienol (Figure 5B) or 200 mM β-lactose (Figure 5C), results in a marked reduction in galectin-3 expression and a corresponding reduction in fibronectin polymerization and fibrillar formation. Quantification of treatment effects shown in Figures 5A, 5B, and 5C demonstrates that treatment with either 6 μM γ-tocotrienol or 200 mM β-lactose results in both a significant decrease in extracellular galectin-3 expression and fibronectin fibril formation, as compared with TS/A cells in the vehicle-treated control group (Figure 5D).

Effects of γ-Tocotrienol and β-Lactose on Intracellular Vinculin and F-Actin Reorganization in Highly Malignant TS/A Mammary Tumor Cells: Vehicle-treated control TS/A cells show intracellular vinculin (green) form focal adhesions with the F-actin stress fibers to produce lamellipodial protrusions and creates a cellular shape similar to that of a mesenchymal cell (Figure 6A). The high relative levels of intracellular vinculin (green) serves as a platform for intracellular F-actin (red) focal adhesion formation. Ultimately, this arrangement of vinculin (green) and F-actin (red) creates morphological changes that lead to the production of lamellipodial protrusions, which is a hallmark of epithelial-to-mesenchymal transition (EMT) (14). Treatment with either 6 μM γ-tocotrienol (Figure 6B) or 200 mM β-lactose (Figure 6C) results in a reorganization of vinculin and F-actin in the cytoplasm and a corresponding reduction in lamellipodial protrusions. Quantification of treatment effects shown in Figures 6A, 6B, and 6C demonstrates that treatment with either 6 μM γ-tocotrienol or 200 mM β-lactose results in a significant decrease in the

formation of lamellipodial protrusions, as compared with the highly metastatic TS/A cells in the vehicle-treated control group (Figure 6D).

FRET Assay Analysis of γ-Tocotrienol and β-Lactose Treatment Effects on Galectin-3 Protein-Protein Interaction in Fixed Highly Malignant Human MDA-MB-231 Breast Cancer Cells as Determined by Confocal Microscopy: The FRET assay is a technique that can be used to visualize protein-protein interactions by measuring the transfer of energy between two fluorescent dyes (called a donor and an acceptor fluorophore) when they are positioned very close (within 1 to 10 nM) together. Specifically, when excited by light, a donor fluorophore transfers its energy to a nearby acceptor fluorophore if each is in very close proximally to one another, where their emission and excitation wavelengths overlap, resulting in a decrease in donor fluorescence and an increase in acceptor fluorescence. The efficiency of FRET depends on the distance between the donor and acceptor molecules and the overlap between the donor emission spectrum and acceptor excitation spectrum. Since galectin-3 can undergo oligomerization (up to a pentamer) and crosslink glycosylated ligands to form a dynamic lattice that is associated with EMT and malignant phenotype expression, the FRET assay can be used to determine treatment effects on galectin-3 protein-protein interaction. Fluorescent images from each channel were captured sequentially to prevent cross-talk between channels. Cells in all treatment groups were incubated with FRET donor and acceptor fluorophores conjugated to galectin-3, to visualize oligomer formation. After 1 hour of treatment exposure, cells in all treatment groups were excited at 543 nm and the fluorescence signal was obtained with a red emission filter. Cells in each treatment group were then excited at 488 nm and fluorescence was obtained with a green emission filter. Finally, cells were excited at 488 nm and the FRET fluorescence signal was obtained with a red emission filter.

Results show that MDA-MB-231 cells in the vehicle-treated control group produced an intense fluorescence signal when excited with either 543 nm and paired with red emission filter (Figure 7, top row, left column) or excited with 488 nm and paired with green emission filter (Figure 7, top row, middle column). These findings indicate that both the donor and acceptor galectin-3 fluorophores are present in high levels in the extracellular matrix surrounding these cells. Furthermore, when control cells were excited with 488 nm paired with red emission filter, a relatively intense FRET signal is observed, indicating that the donor and acceptor fluorophores were very closely co-localized (<10 nm) in the extracellular matrix surrounding the vehicle-treated control cells (Figure 7, top row, right column). These results indicate closely associated protein-protein interaction between the donor and acceptor galectin-3 fluorophores exist in a dynamic lattice. In contrast, when fluorescence was measured using the same combination of excitation wavelengths and red and green emission filters, cells in the γ-tocotrienol (Figure 7, middle column, middle row) and β-lactose (Figure 7, middle column, bottom row) treatment groups display a slight decrease in donor and acceptor galectin-3 fluorophores present in the extracellular matrix surrounding these cells. However, cells in both the γ-tocotrienol (Figure 7, middle row, right column) and β-lactose (Figure 7, bottom row, right column) treatment groups displayed nearly a complete absence of FRET fluorescence signaling, as compared to cells in the vehicle-treatment control group (Figure 7, top row, right column), suggesting that there is a treatment-induced decrease in galectin-3 oligomerization and lattice formation in the extracellular matrix surrounding these cells.

Real Time Treatment Effects of γ-Tocotrienol and β-Lactose on Galectin-3 FRET Fluorescent Signaling in Living MDA-MB-231 Breast Cancer Cells Grown in Culture, as Determined with a Fluorescence Plate Reader: In order to confirm and quantify treatment effects on FRET signal

intensity, similar studies were conducted with living MDA-MB-231 cells maintained in culture using a fluorescence plate-reader. Following a 1-hour treatment exposure, cells in either the 15 μM γ-tocotrienol or 200 mM β-lactose group displayed a significant decrease in FRET signaling, as compared to MDA-MB-231 cells in the vehicle-treated control group, respectively (Figure 8A). Following a 6-hour treatment exposure to these same treatments, cells in both the 15 μM γ-tocotrienol or 200 mM β-lactose groups displayed a significant and relatively large decrease in FRET signaling, as compared to cells in the vehicle-treated control group (Figure 8B). These findings provide quantitative evidence supporting the hypothesis that treatment with the galectin-3 inhibitors γ-tocotrienol or β-lactose, causes a significant time-responsive decrease in galectin-3 oligomerization and lattice formation in the extracellular matrix surrounding these cells.

Effects of γ-Tocotrienol and β-Lactose on the Inverse Relationship Between Galectin-3 and Doxorubicin Nuclear Staining in Highly Malignant Mouse TS/A Mammary Tumor Cells: TS/A cells grown in vehicle-treated control media show that doxorubicin levels are undetectable in the nucleus (Figure 9A, left side) and is not present to produce magenta co-localization staining with galectin-3 and DAPI (Figure 9A, right side) in the nucleus of these cells. Treatment exposure to a low dose (2 μM) of doxorubicin show very faint nuclear red fluorescence staining intensity (Figure 9B, left side). Triple staining for doxorubicin (red), galectin-3 (green) and nuclear counterstaining with DAPI (blue), shows there is very little doxorubicin located in the nucleus in these cells, as indicated by very low intensity of magenta produced by the combination of the red and blue fluorophores (Figure 9B, right side). In contrast, treatment with 2 μM doxorubicin in combination with 6 μM γ-tocotrienol shows a relatively large increase in nuclear doxorubicin (red) fluorescence intensity (Figure 9C, left side), and a corresponding increase in nuclear magenta staining (Figure 9C, right side). Similarly, combined treatment with 2 μM doxorubicin and 200 mM β-lactose

result also induced a relatively large increase in doxorubicin (red) nuclear fluorescence staining (Figure 9D, left side) and corresponding increase in the nuclear co-localization of doxorubicin and DAPI (magenta) fluorescence staining (Figure 9D, left side). These findings indicate that combined treatment of doxorubicin with the galectin-3 inhibitors, γ-tocotrienol or β-lactose, induces an increase in nuclear doxorubicin levels in malignant TS/A mammary tumor cells.

DISCUSSION

Results in the present study demonstrate that γ-tocotrienol reversal of EMT in metastatic breast cancer cells is mediated, at least in part, through its inhibitory effects on galectin-3 expression, intra- and extracellular distribution and oligomerization. Specifically, acute exposure to γ-tocotrienol was found to induce a rapid and significant time-responsive decrease in galectin-3 levels in metastatic cells. It was also found that galectin-3 extracellular distribution is widespread in vehicle-treated metastatic control cells, and treatment exposure γ-tocotrienol induces a marked extracellular reorganization of galectin-3 in these cells. Studies also show that treatment with the galectin-3 inhibitors, γ-tocotrienol or β-lactose, induced a significant reduction in galectin-3 expression and a corresponding reversal in EMT as evidence by a reduction in the formation of fibronectin fibrils and lamellipodial protrusions. Experimental results also show that metastatic breast cancer cells treated with either γ-tocotrienol or β-lactose display a significant decrease in galectin-3 FRET signaling, as compared to cells in the vehicle-treated control group, and is reflective of a significant reduction in galectin-3 expression, oligomerization and lattice formation. Studies also show that treatment with doxorubicin in combination with either γ-tocotrienol or β-lactose caused a large relative increase in doxorubicin levels in the nuclei of metastatic breast cancer cells, and suggest that combined therapy with these galectin-3 inhibitors potentiates the anticancer effectiveness of this chemotherapeutic agent. Taken together, these findings demonstrate that γ-tocotrienol induced reversal in metastatic breast cancer cell EMT is mediated by a disruption in the galectin-3 expression and reorganization in galectin-3 distribution. Although biomolecular and imaging experiments support the proposed disruption in protein-protein interactions during galectin-3 inhibition, the findings are limited by the use of *in vitro* cellular models. For instance, protein concentrations, cofactors, post translational modifications,

competing binding partners, cellular crowding, and compartmentalization are not fully reproduced using *in vitro* models. Also, recombinant galectin-3 conjugated to fluorophores may lack modifications and conformations present in the native protein state found within *in vivo* models. Therefore, further studies employing *in vivo* models will be necessary to determine the physiological relevance of this mechanism.

γ-Tocotrienol is a natural isoform in the vitamin E family of compounds that displays potent anticancer activity, Previous studies showed that γ-tocotrienol exerts antiproliferative, apoptotic, autophagic and antioxidant effects against several types of human and murine mammary tumor cell lines (10, 11, 15), and in particular, induces a reversal EMT and metastatic phenotypic behavior (2, 6, 10, 11, 15) in these cells. Cells undergoing EMT are characterized by acquiring mesenchymal phenotypic traits that promotes their migration to other parts of the body (16). Previous research revealed that highly metastatic mouse mammary tumor cells were characterized by EMT, as indicated by the high expression of mesenchymal cell markers (e.g. vimentin) and a corresponding low expression of epithelial cell markers (e.g. cytokeratins), and γ-tocotrienol treatment induced a reversal in the expression of these cell markers (6). Other studies showed that γ-tocotrienol-induced reversal in EMT was mediated in part by a significant suppression in Wnt/β-catenin and Hedgehog (2, 8). Furthermore, it is now well established that galectin-3 promotes EMT by activating various signaling pathways, which regulate key transcription factors and genes involved in EMT. Results in the present study supports and extends these previous findings, and further demonstrate that γ-tocotrienol-induced reversal of EMT is associated with an inhibition in galectin-3 expression and a reorganization of galectin-3 distribution.

Galectin-3 is a soluble glycan-binding protein that is present in both the intra- and extracellular domains which interacts with numerous glycoproteins and glycolipids to regulate a

wide range of biological processes including EMT (17). Cytosolic galectin-3 can directly bind to glycans through protein-protein bindings sites located in its CRD (18). Likewise, once galectin-3 is secreted it can then bind to extracellular glycans to modulate membrane function and receptor second messenger signaling, which has a positive feedback effect on its own expression and function (19). The process of EMT involves changes in either an increased or decreased in glycosylation patterns of proteins and lipids, ultimately leading to an increase in metastatic phenotypic behavior (20). Treatment of metastatic mammary tumor cells with 5 μM γ-tocotrienol was found to induce a significant time-responsive decrease in galectin-3 levels in metastatic cells. β-lactose is a well-established competitive inhibitor of extracellular galectin-3 carbohydrate binding (12). Computer assisted Schrodinger docking studies show that both galectin-3 inhibitors, γ-tocotrienol and β-lactose, display similar binding sites within the galectin-3 CRD region that appear to be involved in mediating their inhibitory effects.

Metastatic breast cancer cells are characterized by galectin-3 binding to specific branched N-glycans on the cell surface of metastatic cells, which then triggers F-actin remodeling to form fibrillar adhesions that play an essential role in cancer cell migration, whereas intracellular vinculin form focal adhesions with the F-actin stress fibers to produce lamellipodial protrusions similar to that in mesenchymal cells (21). Studies show that treatment with either γ-tocotrienol or β-lactose results in a significant decrease in galectin-3 expression, fibronectin fibril formation and lamellipodial protrusions in metastatic breast cancer cells, a clear demonstration of EMT reversal and attenuation of the metastatic phenotype.

The FRET assay is an extremely sensitive technique that can be used to analyze protein-protein interactions at very close proximity in the range of 1 to 10 nM (22). Since galectin-3 can undergo oligomerization (up to a pentamer) (23), and crosslink glycosylated ligands to form a

dynamic lattice that is associated with EMT and malignant phenotype expression, the FRET assay utilized to determine treatment inhibitory effects of γ-tocotrienol or β-lactose on galectin-3 protein-protein interaction in metastatic MDA-MB-231 human breast cancer cells. Results show that cells grown in vehicle-treated control media displayed a robust FRET signal, as determined using confocal microscopy. These findings were then confirmed and quantified in similar studies conducted in real time in living MDA-MB-231 cells maintained in culture using a fluorescence plate-reader. Furthermore, treatment with either γ-tocotrienol or β-lactose resulted in a large relative decrease in FRET signaling. The significance of these results demonstrates that galectin-3 (donor fluorophore) closely associated protein-protein bonds with surrounding galectin-3 (donor fluorophore). However, it is also possible that these treatment effects may induce changes in the binding of galectin-3 with surrounding glycoproteins and/or glycolipids. If such an event would occur, this could bring the donor and acceptor galectin-3 molecules closer together or move them apart, and bring about a change in FRET signaling. Nevertheless, because the energy transfer for the donor to the acceptor is dependent on their close proximity, the current finding confirm that the protein-protein interactions are occurring at a specific time and location within the cell (24).

Doxorubicin is a potent anticancer chemotherapeutic agent that concentrates in the nucleus of tumor cells, where it induces double stranded breaks in DNA and ultimately disrupts normal DNA replication, transcription, and cell proliferation (25). Since galectin-3 expression is found to be relatively much higher in malignant breast cancer cell types (TS/A, +SA and MDA-MB-231 cells), as compared to nonmalignant cells (MCF-7), studies were conducted to examine the effects of the galectin-3 inhibitors, γ-tocotrienol and β-lactose, on the inverse relationship between extracellular galectin-3 expression and distribution, and intracellular doxorubicin nuclear levels in malignant TS/A mammary tumor cells. The present results show that combined treatment of

doxorubicin with either of these galectin-3 inhibitors, induces a relatively large increase in nuclear doxorubicin levels in these cells, which may indicate galectin-3 inhibition could be utilized in conjunction with doxorubicin chemotherapy. Additional studies are required to investigate this possibility.

In summary, γ-tocotrienol displays a duel binding profile with galectin-3, and following treatment of metastatic breast cancer cells with γ-tocotrienol results in a significant decrease in galectin-3 expression and oligomerization, as well as reorganization in the galectin-3 extracellular distribution, and a corresponding reversal in EMT, indicated by a reduction in fibronectin fibril and lamellipodial protrusion formation. Resonance transfer between fluorophores conjugated to galectin-3 further confirms these interactions, underscoring the intricate role of γ-tocotrienol in modulating galectin-3 functionality in metastatic breast cancer cells. Furthermore, combined treatment of γ-tocotrienol with doxorubicin induced a relatively large increase in the levels of doxorubicin in the nucleus of metastatic breast cancer cells, the primary site of action for this anticancer chemotherapeutic agent. Taken together, these and other findings suggest that γ-tocotrienol therapy may provide significant benefit in the treatment of highly malignant breast cancer that is characterized by galectin-3-induced promotion of EMT.

MATERIALS AND METHODS

Protein-Ligand Docking: The Schrödinger molecular docking software (Schrodinger, New York, NY, USA) was used to investigate interactive binding sites on the galectin-3 protein that form a docking complex with β-lactose and γ-tocotrienol. The crystal structure named 5EXO, which refers to human galectin-3 CRD in complex with methyl 2-O-acetyl-3-O-(2H-chromene-3-yl-methyl)-a-D-galactopyranoside, is a highly selective, high-affinity inhibitor of human galectin-3,

was obtained from the Worldwide Protein Data Bank (WWPDB) (26).

Reagents and Antibodies: Chemicals and reagents utilized in this study were purchased from Sigma-Aldrich (St. Louis, MO, USA), unless otherwise indicated. γ-Tocotrienol was obtained from Davos Life Science Sdn Bhd (Selangor, Malaysia). β-lactose (#H54447) was purchased from Thermo Fisher Scientific (Waltham, MA, USA). Galectin-3 (#B2C10) and vinculin (#7F9) antibodies were obtained from Santa Cruz Biotechnology (Dallas, TX, USA) and fibronectin antibody (#ab45688) was obtained from Abcam (Waltham, MA, USA). Goat anti-mouse antibody (#NEF822001EA) used for Western blot analysis was purchased from PerkinElmer Biosciences (Boston, MA, USA). TGX Stain-Free FastCast Acrylamide Kit 12% (#1610185) was purchased from Bio-Rad (Hercules, CA, USA) for use in Stain-Free Western Blot analysis. Goat anti-rabbit and anti-mouse secondary antibodies used for immunocytochemistry were obtained from Invitrogen (Carlsbad, CA, USA). ActinRed 555 ReadyProbes (#R37112) reagent were purchased from Invitrogen (Carlsbad, CA, USA). Antifade mounting medium with DAPI (#H-1200) was purchased from Vectashield (Vector Laboratories Inc., CA, USA). Galectin-3-Alexa 488 and galectin-3-Alexa 555 were purchased from Creative Biostructure (Shirley, NY, USA).

***Cell Lines and Culture Conditions*:** The murine +SA mammary epithelial cell line was originally isolated from a mammary adenocarcinoma that spontaneously developed in a BALB/c female mouse (27, 28). This cell line is recognized for its highly malignant characteristics, being estrogen-independent and demonstrating anchorage-independent growth when cultured in soft agar gels. Culture and passaging methodology related to maintaining these cell lines have been previously described in detail (10). Human metastatic MDA-MB-231 and the mouse metastatic TS/A mammary tumor cell line were purchased from Sigma-Aldrich (St. Louis, MO, USA). Stock cell lines were maintained in "growth media" containing RPMI-1640 medium supplemented with 10%

fetal bovine serum (FBS), 100 U/mL penicillin, 0.1 mg/mL streptomycin, and 10 µg/mL insulin), and cultured in a humidified incubator at 37°C with an atmosphere of 95% air and 5% CO_2 and fed fresh medium every other day. For isolation and experimentation, stock cells were selected for use at approximately 70% confluency, rinsed in sterile calcium and magnesium-free phosphate-buffered saline (PBS), and then treated with 0.05% trypsin and 0.025% ethylenediaminetetraacetic acid (EDTA) in PBS for 4 minutes at 37°C. Afterwards, the enzymatic activity of trypsin was neutralized by adding an equal volume of bovine calf serum (BCS). Cells were then collected, centrifuged, resuspended in fresh medium, and counted manually using a hemocytometer.

Experimental Treatments: A stock solution of γ-tocotrienol was prepared as previously described in detail (15). Briefly, a given concentration of lipid soluble γ-tocotrienol was dissolved in 100 µL of absolute ethanol and then combined with sterile 10% bovine serum albumin (BSA) in sterile water and incubated overnight at 37°C with gentle agitation. The prepared stock solution was then utilized to formulate various concentrations of treatment media, ensuring that the final ethanol concentration remained below 0.1% across all experimental groups. For use in experimentation, human MDA-MB-231 cell lines were cultured in RPMI-1640 medium supplemented with 2% fetal bovine serum (FBS), 100 U/mL penicillin, 0.1 mg/mL streptomycin, and 10 µg/mL insulin, whereas the mouse TS/A and +SA cell line were maintained in serum-free defined media consisting of Dulbecco's modified Eagle's medium (DMEM/F12) supplemented with 10 µg/ml transferrin, 100 U/ml soybean trypsin inhibitor, 100 U/ml penicillin, 0.1 mg/ml streptomycin, 10 ng/ml EGF, and 10 µg/ml insulin. Isolated human and murine cells in their respective control media were then plated at a density of 5 X 10^3 cell/well in 96 well plates or 1 X 10^6 cells/100mm culture plates and then returned to the incubator to allow cells to attach overnight (Day 0). The following day (Day 1), cells were divided into different treatment groups, control media was

removed, and then replaced with their respective fresh treatment media. Treatment doses of γ-tocotrienol used in experimentation were previously found to be in the subeffective dose range as determined in previously published dose-response viability studies for each cell line (2, 7, 9). β-Lactose is a weak, natural, competitive inhibitor of galectin-carbohydrate binding and is commonly used as an established negative control for galectin-3 carbohydrate-binding and intra- and extracellular distribution, and treatment doses of β-lactose has not been found to significantly affect cell proliferation and/or viability of cancer cells (11).

Fluorescent Immunocytochemistry: Culture slides were pretreated with growth media supplemented with bovine plasma fibronectin to promote cellular adhesion (29). Cells were then isolated with trypsin, counted, and then resuspended in control media as described above. Isolated cells were then seeded at a density of 2-4 X 10^4 cells/chamber in BD Falcon eight-chamber glass culture slides (San Jose, CA, USA), returned to the incubator and allowed to attach overnight. The following day, media was removed, cells were washed in sterile PBS, and then fed their respective treatment media for a designated incubation period. Media was changed every day for all cells in their respective treatment groups. Afterwards, cells were washed in ice-cold PBS, fixed in 4% formaldehyde/PBS for 6 minutes. Fixed cells were then washed in PBS and blocked with 5% goat serum in PBS for 1 hour at room temperature. Magnesium and calcium were added to the PBS washing buffer and used before galectin-3 staining to retain adhesion and galectin-3 integrity. Cells in each treatment group were then further subdivided and incubated with specific primary antibodies for vinculin (1:300 dilution), galectin-3 (1:400 dilution), and fibronectin (1:200 dilution) at 4°C in PBS containing 5% goat serum, as described in their respective Figure Legends. Permeabilization with 0.4% triton X-100 in PBS was only used in the primary and secondary antibody solution for vinculin staining. For fibronectin staining, 0.4% triton X-100 was added to

the washing buffer and only used prior to primary and secondary incubation. Permeabilization was not needed for extracellular galectin-3 staining, since permeabilization resulted in a disruption of extracellular galectin-3 distribution and concentration. Cells were then washed 3 times in ice-cold PBS, and then incubated with fluorescein- or rhodamine-conjugated secondary antibody (1:2000) in PBS containing 5% goat serum for 1 hour at room temperature. F-actin staining was performed using ActinRed 555 ReadyProbes reagent (Invitrogen) following the protocol provided by the manufacturer. All cells were then washed 3 times in ice-cold PBS and mounted with Vectashield medium containing DAPI (Vector Laboratories Inc., CA, USA). The fluorescent images were captured using LSM Pascal confocal microscope (Carl Zeiss Microimaging Inc., Thornwood, NY, USA).

Stain-free Western Blot Analysis: Following experimentation, cells were isolated with trypsin, and whole cell lysates were prepared as previously described above (15). The Bio-Rad protein assay kit (Bio Rad, Hercules, CA, USA) was used to calculate protein concentration in each sample. Equal amounts (3 µg/lane of each protein sample was loaded into each well and then subjected to electrophoresis using 12% Bio-Rad TGX stain-free fastcast acrylamide gels (Bio-Rad Hercules, CA). Gels were then UV-activated (45 seconds) post-electrophoresis in a BioRad ChemiDoc Touch Imaging System to visualize total protein in each lane. Total protein in each individual lane was then used to normalize protein loading as described by the Stain-Free protocol instructions provided by Bio-Rad. As such, Stain-free Western Blot analysis eliminates the need to include the use of housekeeping proteins (actin, α-tubulin, etc.) for normalization of specific protein bands in each lane. Gel proteins were then transferred onto a single 8 x 6.5 inch 0.2 µm polyvinylidene fluoride (PVDF) membrane (#1620177; Bio-Rad, Hercules, CA, USA) using a Trans-Blot Cell (Bio-Rad, Hercules, CA, USA) at 270 mA for 3 hours at 4°C. After transfer,

membranes were blocked with a 2% BCS buffer solution containing 10 mM Tris-HCl, 50 mM NaCl, and 0.1% Tween 20 (pH 7.4, TBST) for 2 hrs. The membranes were then incubated with a primary antibody against galectin-3, diluted at 1:1000 in 2% BCS in tris-buffered saline and Tween (TBST) for 12 hours at room temperature. Following primary antibody incubation, membranes were washed 5 times in TBST and subsequently incubated with secondary goat anti-mouse antibodies diluted 1:5000 in 2% BCS in TBST for 2 hours at room temperature. The membranes were then washed an additional five times in TBST before exposure to SuperSignal West Pico PLUS chemiluminescent substrate (#34580) from Life Technologies (Carlsbad, CA, USA). The buffer washes and antibody incubations were conducted utilizing Freedom Rocker BlotBot automation (Next Advance, Inc., Troy, NY, USA). Chemiluminescence optical density (O.D.) was visualized with the ChemiDoc MP system and normalized to total in-lane protein using Image Lab software (Image Lab 6.0.1; Bio-Rad). Precision plus protein molecular weight dual-color standard (Protein Ladder) (#1610377; Bio-Rad) was included in each Western blot analysis. All experiments were conducted in triplicate and a representative image is presented in the Figures.

Confocal Microscopy: Fluorescent images were acquired using the LSM Pascal confocal microscope (Carl Zeiss Microimaging Inc., Thornwood, NY, USA). Areas of fluorescence staining were acquired in each well in all treatment groups. Fluorescence from each channel was captured sequentially to prevent cross-talk between channels. The green (Alexa 488 or fluorescein) and red fluorophores (Alexa 555, ActinRed 555, or Rhodamine) were exited with a 488-nm argon-ion and a 543 nm helium neon laser with green and red emission filters, respectively. FRET signaling was detected using the 488 nm argon-ion laser for excitation and red emission filters. Green, red, blue, and merged color images were generated using ZEN software (Zeiss).

Microplate FRET Measurement: Cells in each treatment group were plated at a density of 5 X 10^3 per well in 96-well plates (Nunc) and incubated overnight to allow them to attach to the plates. Cells were then washed 3 times with PBS and then treated with galectin-3-Alexa 488 and/or galectin-3-Alexa 555 (2 μM) fluorophores and incubated for 12 hours. Plates were then again washed 3 times with PBS, and each well exposed to their respective treatments. Fluorescence from living cells in each treatment group was obtained in each well using a Tecan (Männedorf, Switzerland) fluorescent plate reader. Green fluorescence, red fluorescence, and FRET signals were read alternatively using an excitation filter with specific wavelengths as previously described (22). Specifically, Green fluorescence, red fluorescence, and FRET signal were read alternatively using a 485-nm (bandpass 9 nm) excitation filter with a 535-nm (bandpass 20 nm) emission filter, a 545-nm (bandpass 9 nm) excitation filter with a 620-nm (bandpass 20 nm) emission filter, and a 485-nm (bandpass 9 nm) excitation filter with a 620-nm (bandpass 20 nm) emission filter, respectively. Fluorescence signals from each well were measured with the fluorescence microplate reader to quantify FRET signaling over time. The FRET signal obtained from the fluorescence microplate reader is more sensitive than that obtained with the confocal microscope because it has a much narrower bandwidth and is able to detect real time FRET signaling in living cells.

Statistical Analysis: Differences among treatment groups were assessed using one-way analysis of variance (ANOVA) followed by Dunnett's Multiple Comparison Test. A *p*-value of less than 0.05% was considered statistically significant, as compared to their respective control group, or as described in the Figure legends.

ACKNOWLEDGEMENTS

The authors would also like to thank Dr. Karen P. Briski for her generous assistance and use of the laser confocal microscope.

AUTHOR CONTRIBUTION

Jessie J. Grazier designed and conducted all experiments, including data acquisition and analysis, and drafted the manuscript. Paul W. Sylvester obtained the necessary materials and reagents for the study and contributed to manuscript editing and revision. Both authors approved the final version of the manuscript.

FUNDING

This research was supported in part by a grant from the Louisiana Cancer Foundation and the Mark and Mildred Maurer Cancer Research Enhancement Endowed Fund.

DATA AVAILABILITY

All data generated or analyzed during this study was conducted at the University of Louisiana Monroe. This includes data from Schrödinger molecular docking outputs, stain-free western blot source files generated in Image Lab software, confocal microscopy images generated in ZEN Zeiss Microscopy software, and FRET microplate reader datasets generated in I-control 2.0 software. The final data analysis is included in this article. Additional raw data or intermediate analysis files are available from the corresponding author upon request.

CONFLICT OF INTEREST:

There is no conflict of interest.

REFERENCES

1. Fortuna-Costa A, Gomes AM, Kozlowski EO, Stelling MP, Pavao MS. Extracellular galectin-3 in tumor progression and metastasis. Front Oncol. 2014;4:138.

2. Ahmed RA, Alawin OA, Sylvester PW. gamma-Tocotrienol reversal of epithelial-to-mesenchymal transition in human breast cancer cells is associated with inhibition of canonical Wnt signalling. Cell Prolif. 2016;49(4):460-70.

3. Boutas I, Potiris A, Makrakis E, Messaropoulos P, Papaioannou GK, Kalantaridou S. The expression of Galectin-3 in breast cancer and its association with metastatic disease: a systematic review of the literature. Mol Biol Rep. 2021;48(1):807-15.

4. Liu FT, Rabinovich GA. Galectins as modulators of tumour progression. Nat Rev Cancer. 2005;5(1):29-41.

5. Zhao Q, Guo X, Nash GB, Stone PC, Hilkens J, Rhodes JM, et al. Circulating galectin-3 promotes metastasis by modifying MUC1 localization on cancer cell surface. Cancer Res. 2009;69(17):6799-806.

6. Ayoub NM, Akl MR, Sylvester PW. Combined gamma-tocotrienol and Met inhibitor treatment suppresses mammary cancer cell proliferation, epithelial-to-mesenchymal transition and migration. Cell Prolif. 2013;46(5):538-53.

7. Grazier JJ, Sylvester PW. Role of Galectins in Metastatic Breast Cancer. In: Mayrovitz HN, editor. Breast Cancer. Brisbane (AU)2022.

8. Ahmed R. and Sylvester PW. γ-Tocotrienol reversal of epithelial-to-mesenchymal transition in human breast cancer cells is mediated through a suppression of canonical Wnt and Hedgehog signaling pathways. : Tech Publications; 2018.

9. Sylvester PW, Sultana T, Aldabaan N, Anwar MR, Grazier JJ. Intracellular Mechanisms Involved in Mediating gamma-Tocotrienol Reversal of Epithelial-to Mesenchymal Transition (EMT) in Breast Cancer Cells. . In: Watanabe HS, editor. Horizons in Cancer Research. 78: Nova Publishers; 2021.

10. McIntyre BS, Briski KP, Gapor A, Sylvester PW. Antiproliferative and apoptotic effects of tocopherols and tocotrienols on preneoplastic and neoplastic mouse mammary epithelial cells. Proc Soc Exp Biol Med. 2000;224(4):292-301.

11. McIntyre BS, Briski KP, Tirmenstein MA, Fariss MW, Gapor A, Sylvester PW. Antiproliferative and apoptotic effects of tocopherols and tocotrienols on normal mouse mammary epithelial cells. Lipids. 2000;35(2):171-80.

12. Nieminen J, Kuno A, Hirabayashi J, Sato S. Visualization of galectin-3 oligomerization on the surface of neutrophils and endothelial cells using fluorescence resonance energy transfer. J Biol Chem. 2007;282(2):1374-83.

13. Argueso P, Mauris J, Uchino Y. Galectin-3 as a regulator of the epithelial junction: Implications to wound repair and cancer. Tissue Barriers. 2015;3(3):e1026505.

14. Machesky LM. Lamellipodia and filopodia in metastasis and invasion. FEBS Lett. 2008;582(14):2102-11.

15. Tiwari RV, Parajuli P, Sylvester PW. gamma-Tocotrienol-induced autophagy in malignant mammary cancer cells. Exp Biol Med (Maywood). 2014;239(1):33-44.

16. Foroni C, Broggini M, Generali D, Damia G. Epithelial-mesenchymal transition and breast cancer: role, molecular mechanisms and clinical impact. Cancer Treat Rev. 2012;38(6):689-97.

17. Perez-Moreno E, Oyanadel C, de la Pena A, Hernandez R, Perez-Molina F, Metz C, et al. Galectins in epithelial-mesenchymal transition: roles and mechanisms contributing to tissue repair, fibrosis and cancer metastasis. Biol Res. 2024;57(1):14.

18. Vladoiu MC, Labrie M, St-Pierre Y. Intracellular galectins in cancer cells: potential new targets for therapy (Review). Int J Oncol. 2014;44(4):1001-14.

19. Hughes RC. Secretion of the galectin family of mammalian carbohydrate-binding proteins. Biochim Biophys Acta. 1999;1473(1):172-85.

20. Pucci M, Malagolini N, Dall'Olio F. Glycobiology of the Epithelial to Mesenchymal Transition. Biomedicines. 2021;9(7).

21. Nangia-Makker P, Hogan V, Raz A. Galectin-3 and cancer stemness. Glycobiology. 2018;28(4):172-81.

22. Wan Q, Mouton SN, Veenhoff LM, Boersma AJ. A FRET-based method for monitoring structural transitions in protein self-organization. Cell Rep Methods. 2022;2(3):100184.

23. Ahmad N, Gabius HJ, Andre S, Kaltner H, Sabesan S, Roy R, et al. Galectin-3 precipitates as a pentamer with synthetic multivalent carbohydrates and forms heterogeneous cross-linked complexes. J Biol Chem. 2004;279(12):10841-7.

24. van der Ploeg R, Goudelis ST, den Blaauwen T. Validation of FRET Assay for the Screening of Growth Inhibitors of Escherichia coli Reveals Elongasome Assembly Dynamics. Int J Mol Sci. 2015;16(8):17637-54.

25. Bisht A, Avinash D, Sahu KK, Patel P, Das Gupta G, Kurmi BD. A comprehensive review on doxorubicin: mechanisms, toxicity, clinical trials, combination therapies and nanoformulations in breast cancer. Drug Deliv Transl Res. 2025;15(1):102-33.

26. Collins PMaB, H. Crystal structure of Human galectin-3 CRD in complex with methyl 2-O-acetyl-3-O-(2H-chromene-3-yl-methyl)-a-D-galactopyranoside inhibitor. . Worldwide Protein Data Bank. 2016(PDB Entry-5EXO).

27. Anderson LW, Danielson KG, Hosick HL. Metastatic potential of hyperplastic alveolar nodule derived mouse mammary tumor cells following intravenous inoculation. Eur J Cancer Clin Oncol. 1981;17(9):1001-8.

28. Danielson KG, Anderson LW, Hosick HL. Selection and characterization in culture of mammary tumor cells with distinctive growth properties in vivo. Cancer Res. 1980;40(6):1812-9.

29. Lagana A, Goetz JG, Cheung P, Raz A, Dennis JW, Nabi IR. Galectin binding to Mgat5-modified N-glycans regulates fibronectin matrix remodeling in tumor cells. Mol Cell Biol. 2006;26(8):3181-93.

FIGURE LEGENDS

Figure 1: Schrödinger docking analysis of γ-tocotrienol and β-lactose within the galectin-3 carbohydrate recognition domain (CRD) and hydrophobic binding pocket. **A)** Chemical structure of γ-tocotrienol is found in Figure 1A, Top. γ-Tocotrienol is found to preferentially bind to the critical amino acid residues situated within the CRD (Figure 1A, Middle). The binding affinity of γ-tocotrienol within the CRD appears to be further enhanced by the presence of a hydrophobic binding pocket within galectin-3, which accommodates the hydrophobic tail of γ-tocotrienol. Three-dimensional docking with galectin-3 and γ-tocotrienol is shown in Figure 1A, Bottom. **B)** The chemical structure for β-lactose is shown in Figure 1B, Top. The interaction of β-lactose within the galectin-3 CRD is shown in Figure 1B, Middle, where it is found to primarily form hydrogen bonds with galectin-3 amino acids ARG, and GLU. Three-dimensional docking between galectin-3 and β-lactose is shown in Figure 1B, Bottom.

Figure 2: Stain-free Western blot analysis was utilized to evaluate the expression of galectin-3 following a 0-36-hour (hr) treatment exposure to 5 μM γ-tocotrienol (γ-T^3). **A)** Each lane was loaded with 3 μg of cell lysate. Stain-free visualization of total protein in each lane of the whole gel is shown prior to transblot membrane transfer. Total protein per lane was then later used to normalize specific galectin-3 staining following Western blot analysis. **B)** Western blot analysis of galectin-3 expression in highly metastatic mouse +SA cells following a 0-36 hr treatment exposure to 5 μM γ-T^3. **C)** Densiometric analysis of Western blot galectin-3 expression was normalized against the total protein in each individual treatment group's respective lane. Vertical bars indicate the mean $\pm$ S.E.M. in galectin-3 expression in +SA cells throughout the 0-36 hr treatment period. *p<0.05, **p<0.01 and ***p<0.005, as compared to galectin-3 levels in

+SA cells in the 0 hr vehicle-treatment control group. Original blots/gels are presented in Supplementary Figure 1.

Figure 3: A) In the absence of Triton X-100 (0% Triton X-100), immunocytochemical antibodies are unable to gain access to the intracellular targets, resulting in only the visualization of galectin-3 (green) located in the extracellular matrix surrounding. **B)** The lack galentin-3 intracellular visualization in the absence of Triton X-100 treatment is further evidenced by the lack of galectin-3 (green) co-localized with DAPI (blue) in the nucleus of these cells. **C)** Treatment with 0.4% Triton X-100 prior to immunocytochemical analysis, was found to result in the visualization of intracellular galectin-3 (green), as evidenced by its **D)** co-localized with DAPI (blue) in the nucleus. However, pretreatment with Triton X-100 also resulted in the "washing away" of extracellular galectin-3, as evidenced by the absence of galectin-3 visualization in the extracellular matrix of +SA tumor cells. Magnification 20X.

Figure 4: A) Effects of a 24-hour exposure to 5 μM γ-tocotrienol on extracellular galectin-3 (green) distribution in +SA cells. **A)** Vehicle-treated control group exhibited a widespread, but uneven distribution of galectin-3 (green) within the extracellular matrix, whereas **B)** Treatment with γ-tocotrienol resulted in the redistribution of galectin-3 (green) characterized by a defuse distribution of galectin-3 among all cells, but a corresponding concentrated extracellular galectin-3 distribution around only a few individual cells. ImageJ was used to transform the DAPI (blue) and galectin-3 (green) channels shown above in the **C)** vehicle-treated control group and **D)** γ-tocotrienol treated group so that the distribution of extracellular galectin-3 (green) could be visualized in greyscale for structural assessment. Cell nuclei were visualized with DAPI (blue)

counterstaining. Magnification 63X. Statistical quantification of galectin-3 distribution is presented in Supplementary Figure 2.

Figure 5: Effects of γ-tocotrienol and β-lactose on extracellular galectin-3 expression and fibronectin fibril formation and in highly malignant TS/A mammary tumor cells: **A)** TS/A cells in the vehicle-treated control group display tightly formed fibronectin (red) fibrils surrounding a lattice of extracellular galectin-3 (green). **B)** Treatment with either 6 μM γ-tocotrienol (γT3) or **C)** 200mM β-lactose (βLac) results in a relatively large decrease in both extracellular galectin-3 (green) expression and fibronectin (red) fibril formation, as compared to TS/A cells in the vehicle-treated control group. **D)** Quantification of treatment effects on fibronectin fibril formation shown in Figure 6D. At least 50 cells/well in 3 different wells in each treatment group were randomly selected, and then used for statistical analysis. Vertical bars indicate the mean $\pm$ S.E.M. of treatment effects on fibronectin fibril formation in TS/A cells. ***$p<0.005$, as compared to galectin-3 levels in metastatic TS/A cells in the vehicle-treated control group. Magnification is 63X.

Figure 6: **A)** Highly metastatic TS/A cells in the vehicle-treated control group display intracellular vinculin (green) is surrounded by F-actin stress fibers on the intracellular cytoplasmic membrane to produce lamellipodial projections and create a cellular shape like that of mesenchymal cells. Treatment with either **B)** 6 μM γ-tocotrienol (γT3) or **C)** 200 mM β-lactose (βLac) results in a reorganization of vinculin in the cytoplasm and a corresponding reduction in the formation of lamellipodial projections. **D)** Quantification of treatment effects on the formation of lamellipodial projections is shown in Figure 6D. At least 50 cells/well in 3 different wells in

each treatment group were randomly selected, and then used for statistical analysis. Vertical bars indicate the mean ± S.E.M. of treatment effects on fibronectin fibril formation in TS/A cells. ***p<0.005, as compared to galectin-3 levels in metastatic TS/A cells in the vehicle-treated control group. Magnification is 63X.

Figure 7: γ-Tocotrienol and β-lactose treatment effects on galectin-3 FRET signal intensity in fixed MDA-MB-231 breast cancer cells as determined by confocal microscopy. MDA-MB-231 cells in the vehicle-treated control group produced an intense fluorescence signal when excited with either 543 nm and paired with red emission filter (top row, left column) or excited with 488 nm and paired with green emission filter (top row, middle column). Excitation of control cells with 488 nm and paired with red emission filter (top row, right column), induced an intense FRET signal, indicating that the donor and acceptor galectin-3 fluorophores are in very close proximity (< 10nm). Treatment with either 15 μM γ-tocotrienol (middle row, right column) or 200 mM β-lactose (bottom row, right column) results in nearly a complete absence of FRET fluorescence signaling intensity, as compared to cells in the vehicle-treatment control group (top row, right column). Magnification 63X.

Figure 8: Effects of γ-tocotrienol and β-lactose on galectin-3 FRET fluorescent signaling in living MDA-MB-231 breast cancer cells grown in culture. **A)** Following a 1-hour treatment exposure, cells in either the 15 μM γ-tocotrienol (γT3) or 200 mM β-lactose (βLac) group displayed a significant decrease in FRET signaling, as compared to cells in the vehicle-treated control (C) group, respectively. **B)** Following a 6-hour exposure to these same treatments, cells in either the 15 μM γ-tocotrienol or 200 mM β-lactose groups displayed a significantly large decrease in FRET signaling, as compared to cells in the vehicle-treated control group. Vertical bars indicate the

mean FRET signal intensity + S.E.M in each treatment group. ***$p < 0.001$ as compared to cells in the vehicle-treated control group.

Figure 9: Treatment effects of γ-tocotrienol and β-lactose on the nuclear co-localization of doxorubicin and galectin-3 in highly metastatic TS/A mammary tumor cells. **A)** Vehicle-treated control cells were found to contain no detectable levels of nuclear doxorubicin (DOX), and a modest amount of extracellular galecting-3 surrounding each cell. **B)** Metastatic TS/A mammary tumor cells treated with 2 μM (DOX) show a low level of nuclear DOX (left side), and a modest amount of extracellular galectin-3 (right side) surrounding these cells. **C)** Combined treatment of 2 μM DOX with 6 μM γ-tocotrienol (γT3) results in a large relative increase in nuclear DOX (red) levels (left side), and a corresponding increase in the nuclear co-localization of doxorubicin and DAPI (magenta) fluorescent staining in these cells (right side). **D)** Combined treatment of 2 μM DOX with 200 mM β-lactose results in a large relative increase in nuclear DOX (left side), and a corresponding increase in the nuclear co-localization of doxorubicin and DAPI (magenta) fluorescent staining in these cells (right side). Cells were not exposed to Triton X-100, so only extracellular galectin-3 is detected. Magnification 63X.

Figure 1

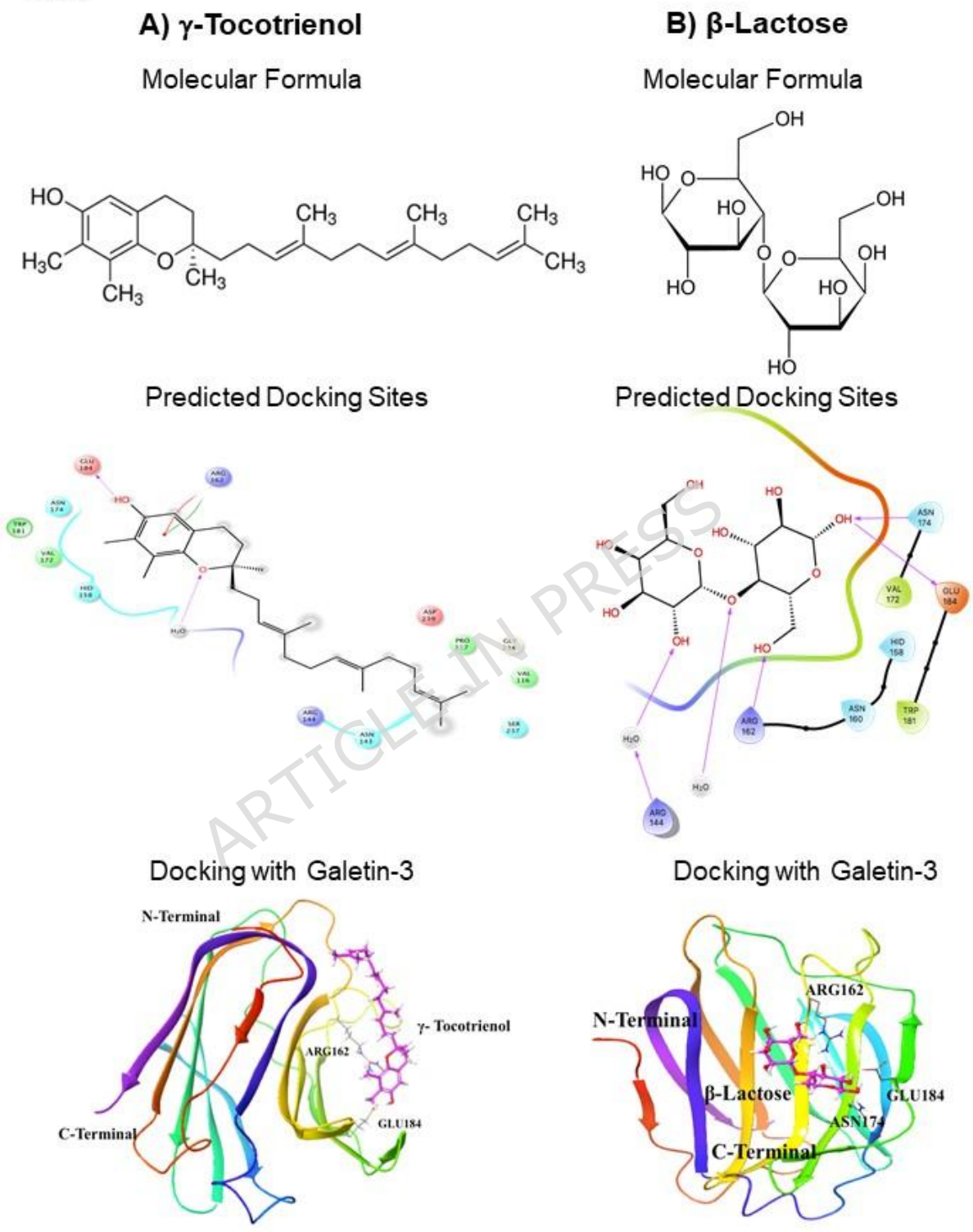

Figure 2

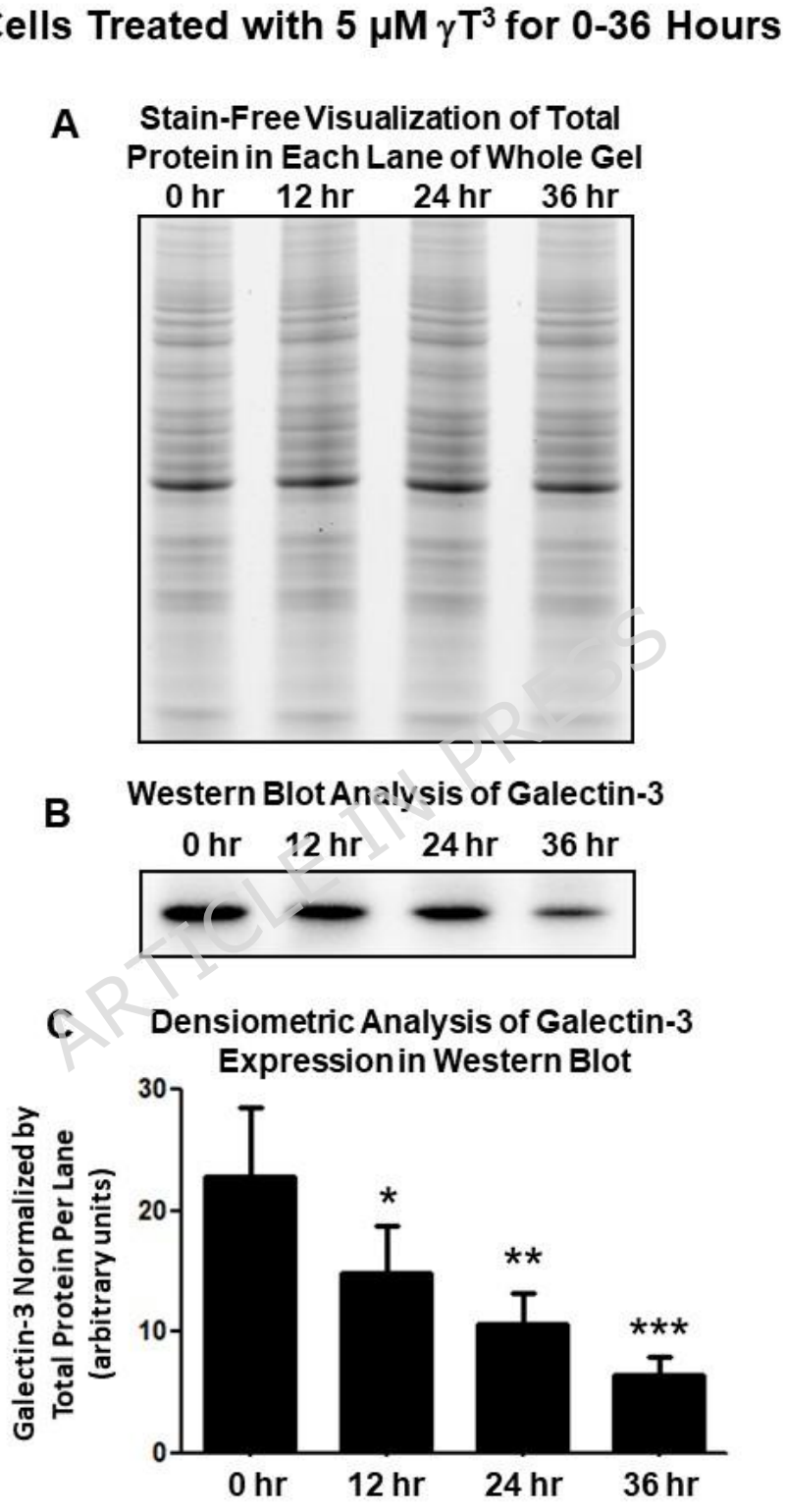

Figure 3

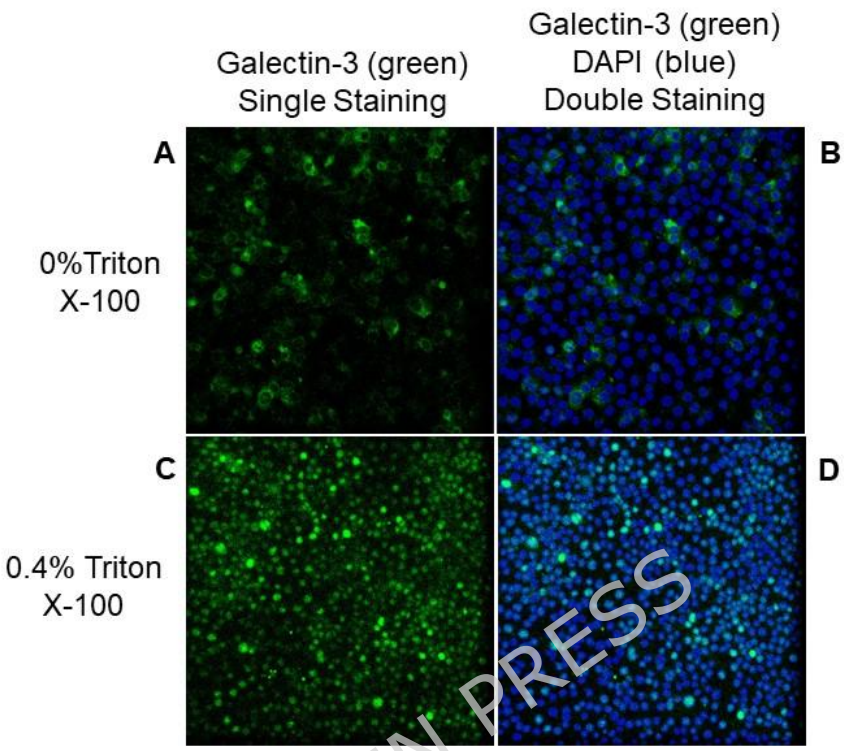

Figure 4

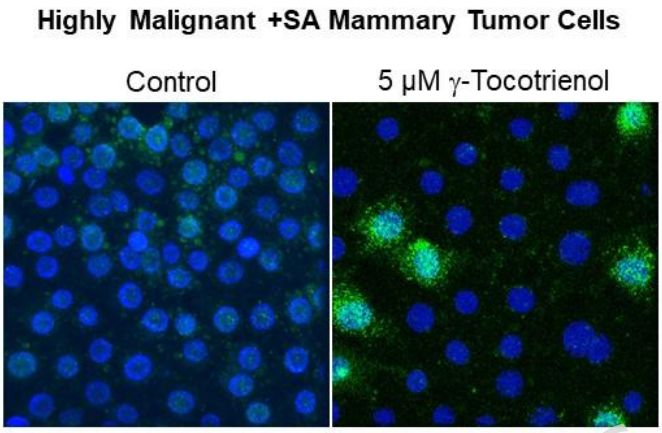

Figure 5

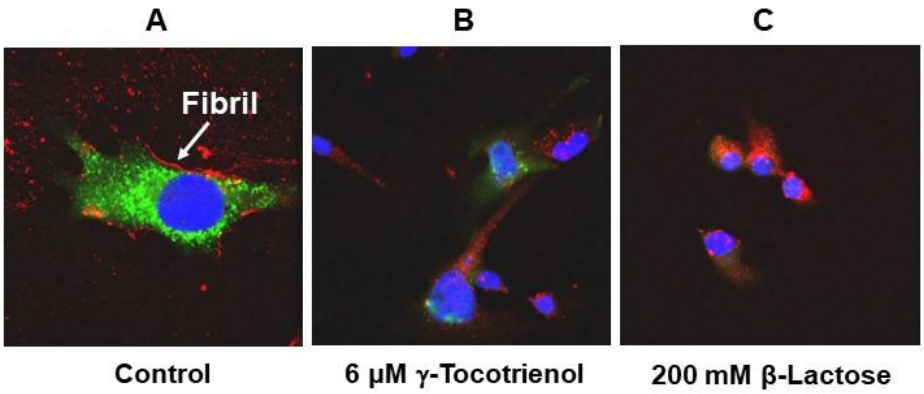

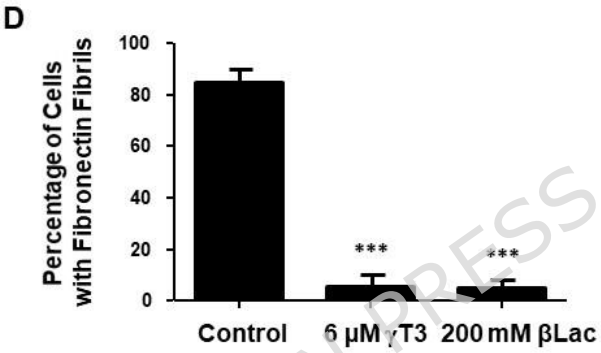

Figure 6

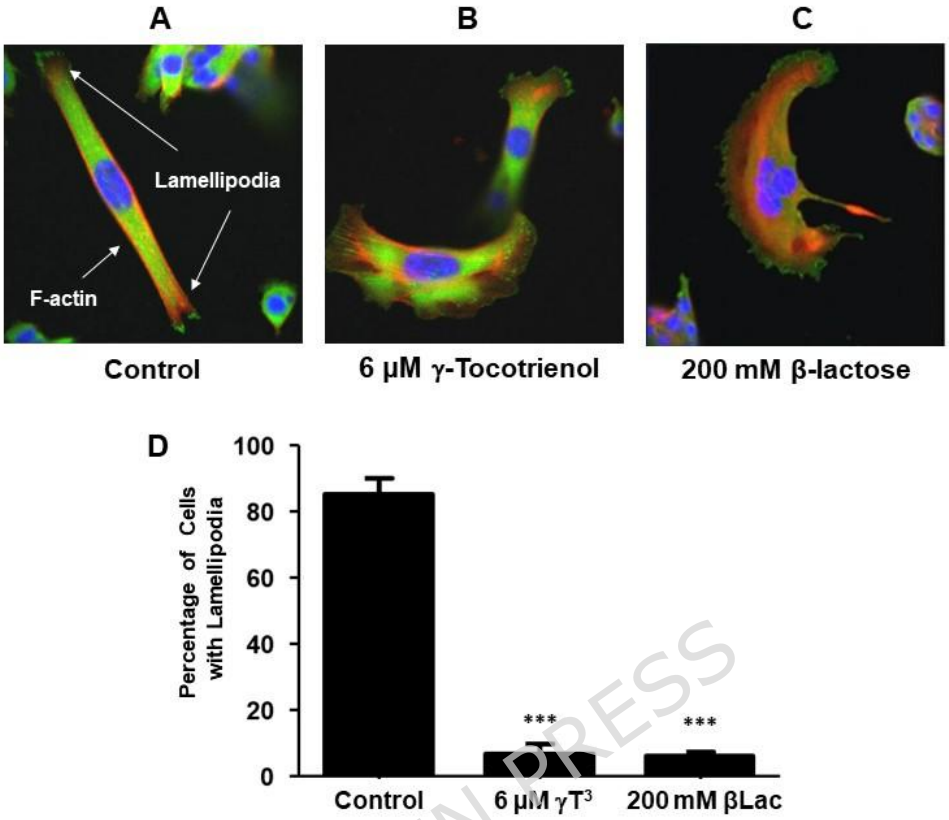

Figure 7

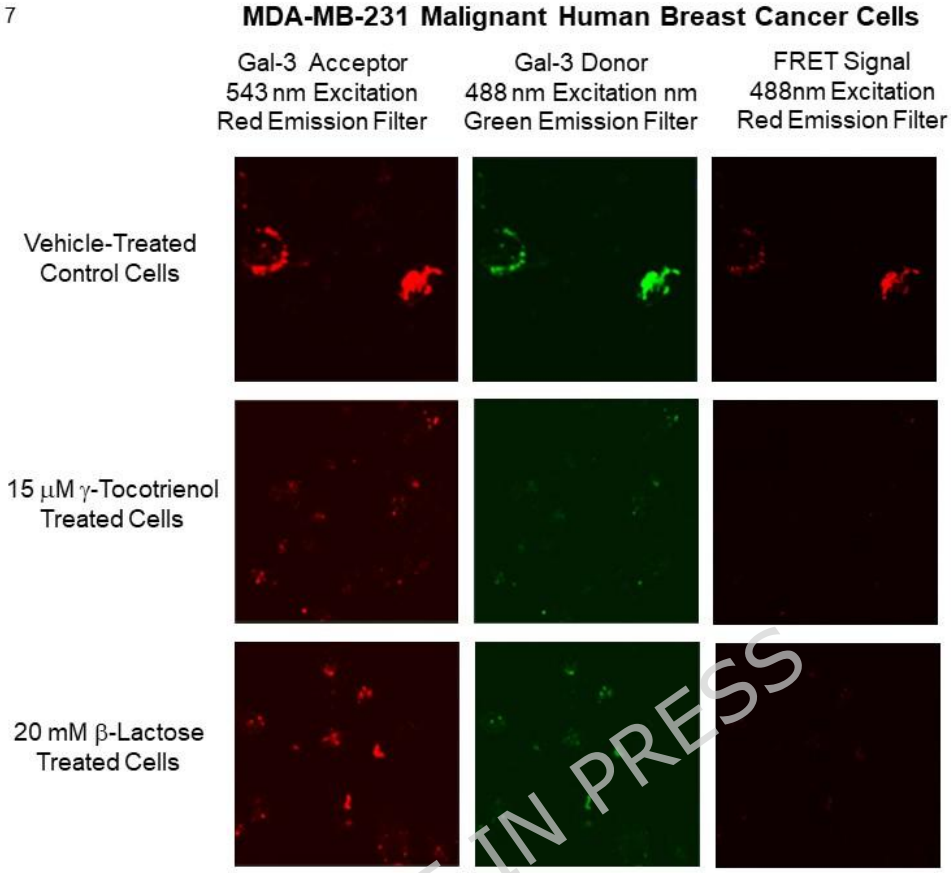

Figure 8

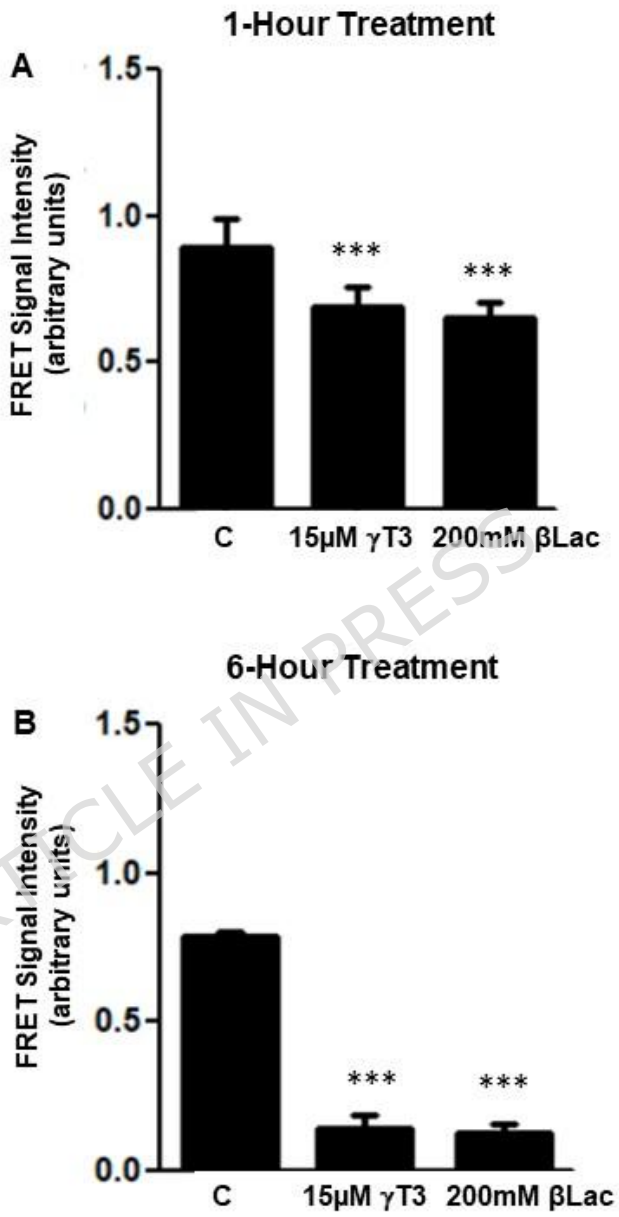

Figure 9